

Electron Refrigeration in the Tunneling Approach

Heinz-Olaf Müller¹ and K. A. Chao

*Department of Physics, Norwegian Institute of Technology, Norwegian University of Science and Technology,
N-7034 Trondheim, Norway*

(June 22, 2021)

The qualities of electron refrigeration by means of tunnel junctions between superconducting and normal-metal electrodes are studied theoretically. A suitable approximation of the basic expression for the heat current across those tunnel junctions allows the investigation of several features of the device such as its optimal bias voltage, its maximal heat current, its optimal working point, and the maximally gained temperature reduction. Fortunately, the obtained results can be compared with those of a recent experiment.

73.40Gk, 73.40Rw, 73.23Hk

I. INTRODUCTION

The properties of the electron refrigerator² are considered in this paper. In conjunction with the SET-thermometer³ it forms a new device⁴ for refrigerating and monitoring electrons at sub-Kelvin temperature. A future on-chip instrument can be used to provide isothermal electrons to other experiments, e.g. in single electronics. The operation is similar to a household refrigerator in so far as the electron temperature, which decouples from the that of the phonons, can be chosen beforehand within a certain domain. Whereas the SET-thermometer, based on “orthodox theory”,⁵ is rather transparent, less effort is taken in case of the refrigerator.⁶

The set-up of the experiment under consideration⁴ is shown schematically in Fig. 1. It consists of a pair of tunnel junctions forming the refrigerator and another pair operating as thermometer. All junctions are connected to the island in the middle whose electrons are dealt with. The leads of the refrigerator are superconducting whereas the thermometer leads are made from a normal metal. The refrigerator double junction is biased by a voltage V close to Δ/e , where Δ is the superconducting gap of its leads. This allows only hot electrons (with an energy larger than the Fermi energy) to leave the island and, vice versa, only cold ones to enter it via the other junction. It is this dispersion which causes electron refrigeration at sub-Kelvin temperature, where the heating by phonons is weak.

On the other hand, the thermometer represents an ultrasmall single-electron double tunnel junction. The thermal dependence of its Coulomb blockade enables the determination of the electron temperature. In general the thermometer is biased too. Since the zero-bias conductance is sufficient³ and advantageous in order to determine the temperature, the bias is usually small and so is the thermometer current as well as the heating by this current.

The tunneling regime of the refrigerator is considered in this paper, which is in contrast to Ref. 6. Due to the large junction resistance Andreev reflections are sup-

pressed and therefore neglected. Following the argument from above, the heating by the thermometer current is also neglected. Furthermore, the refrigerating junctions are thought to be symmetric. This means that there is an equal voltage drop at each junction and the continuity equation for the electric current is fulfilled. In the experiment,⁴ however, a slight asymmetry was found, which is neglected henceforth. Additionally, thermalized electrons are supposed, i.e. a sufficiently high temperature causes a sufficiently short electron-electron scattering time, which in turn causes thermalization of the electrons. As pointed out in Ref. 2 the electron temperature should be above 100 mK to qualify this assumption. An opposite point of view,⁷ however, reveals interesting physics as well.

Our approach starts from the classical formula for the heat current across a NIS junction, namely²

$$P(V) = \frac{1}{e^2 R} \int d\varepsilon N(\varepsilon) (\varepsilon - eV) [f_N(\varepsilon - eV) - f_S(\varepsilon)], \quad (1)$$

where $N(\varepsilon)$ is the density of states on the superconducting side, which is assumed to be the BCS density of states, $N(\varepsilon) = |\varepsilon| \Theta(|\varepsilon| - \Delta) / \sqrt{\varepsilon^2 - \Delta^2}$, and $f_{N,S}(\varepsilon) = 1 / [\exp(\varepsilon / k_B T_{N,S}) + 1]$ is the Fermi distribution function for the normal- and superconducting side, respectively. R is the normal-state junction resistance. The integral (1) is solved in an analytic approximation in Sec. II. Later on conclusions of this result are discussed in Sec. III. It might arise the question, what the advantage of this approximative treatment is if a numerical solution is obtained readily. In our opinion those formulae yield a better insight into the behavior of the refrigerator and its qualities and therefore they are thoroughly worthwhile.

II. CALCULATION

In term of the BCS density of states $N(\varepsilon)$ Eq. 1 can be transformed into

$$\begin{aligned}
P(V) = & \frac{1}{e^2 R} \int_{\Delta}^{\infty} d\varepsilon \frac{\varepsilon^2}{\sqrt{\varepsilon^2 - \Delta^2}} \\
& \times [f_N(\varepsilon - eV) + f_N(\varepsilon + eV) - 2f_S(\varepsilon)] \\
& - \frac{eV}{e^2 R} \int_{\Delta}^{\infty} d\varepsilon \frac{\varepsilon}{\sqrt{\varepsilon^2 - \Delta^2}} \\
& \times [f_N(\varepsilon - eV) - f_N(\varepsilon + eV)]. \quad (2)
\end{aligned}$$

In order to simplify the calculation we apply the following approximation to the Fermi function⁸

$$f(\varepsilon) \approx \Theta(-\varepsilon) + \frac{\text{sgn}(\varepsilon)}{2} e^{-\gamma|\varepsilon|} \quad (3)$$

with $\gamma = 1/(2k_B T \ln 2)$ and $\text{sgn}(\varepsilon) = \varepsilon/|\varepsilon|$, $\text{sgn}(0) = 0$. The value of γ is adjusted to meet

$$\int_0^{\infty} d\varepsilon f(\varepsilon) = \frac{1}{2} \int_0^{\infty} d\varepsilon e^{-\gamma\varepsilon}.$$

In the limit $T \rightarrow 0$ the approximation is exact. Furthermore, it is right at $\varepsilon = 0$. For large $|\varepsilon| \gg k_B T$ the difference to the exact formula is negligible, but for an intermediate energy, $\varepsilon \sim k_B T$ it is not. Hence, we expect this approximation to work out at low temperature, i.e. at $k_B T \ll \Delta$ here. This condition is obeyed fairly good in the experiment.⁴

The main advantage of (3), however, is the possibility to reduce the integrals of (2) to Laplace transformations. In detail we find with

$$\begin{aligned}
f_N(\varepsilon - eV) + f_N(\varepsilon + eV) - 2f_S(\varepsilon) & \approx e^{-\gamma_N \varepsilon} \cosh(\gamma_N eV) \\
& - e^{-\gamma_S \varepsilon}, \\
f_N(\varepsilon - eV) - f_N(\varepsilon + eV) & \approx e^{-\gamma_N \varepsilon} \sinh(\gamma_N eV)
\end{aligned}$$

and⁹

$$\begin{aligned}
g(p) = \mathcal{L}[f(t)](p) & = \int_0^{\infty} dt f(t) e^{-pt}, \\
\mathcal{L}\left[\frac{\varepsilon \Theta(\varepsilon - \Delta)}{\sqrt{\varepsilon^2 - \Delta^2}}\right](\gamma) & = \Delta K_1(\gamma \Delta), \\
\mathcal{L}\left[\frac{\varepsilon \Theta(\varepsilon - \Delta)}{\sqrt{\varepsilon^2 - \Delta^2}}\right](\gamma) & = -\Delta \frac{d}{d\gamma} K_1(\gamma \Delta) \\
& = \frac{\Delta^2}{2} [K_0(\gamma \Delta) + K_2(\gamma \Delta)],
\end{aligned}$$

where $K_\nu(z)$ is the modified Bessel function of ν -th order,

$$\begin{aligned}
P(V) \approx & \frac{\Delta^2}{2e^2 R} \{ [K_0(\gamma_N \Delta) + K_2(\gamma_N \Delta)] \cosh(\gamma_N eV) \\
& - K_0(\gamma_S \Delta) - K_2(\gamma_S \Delta) \} \\
& - \frac{\Delta e V \sinh(\gamma_N eV)}{e^2 R} K_1(\gamma_N \Delta). \quad (4)
\end{aligned}$$

Eq. 4 is the main result of this paper. We are going to discuss it in the next section.

III. DISCUSSION

Following Ref. 6 we consider the limit $\gamma_{N,S} \Delta \gg 1$, $eV = \Delta$ first, which describes the experimental situation to a large extent. In this case the use of the asymptotic expansion¹⁰

$$K_\nu(z) \approx \sqrt{\frac{\pi}{2z}} e^{-z} \left[1 + \frac{4\nu^2 - 1}{8z} \right]$$

simplifies (4) to

$$\begin{aligned}
P(\Delta/e) & \approx \frac{(\pi \ln 2)^{3/2}}{2\pi} \frac{\Delta^2}{e^2 R} \left(\frac{k_B T_N}{\Delta} \right)^{3/2} \\
& \approx 0.51 \frac{\Delta^2}{e^2 R} \left(\frac{k_B T_N}{\Delta} \right)^{3/2}. \quad (5)
\end{aligned}$$

Eq. 5 recovers the temperature dependence $P(\Delta/e) \propto T_N^{3/2}$ of the exact result.⁶ The numerical prefactor, however, is found to be slightly larger (0.48 in Ref. 6). The agreement approves of the introduced approximation (3) and indicates that its accuracy is in the few-percent range.

In a next step (4) can be used to determine the optimal value of the bias voltage V . From the formal derivative of (4) it is found that this value V_{opt} should obey the equation

$$\gamma_N e V_{\text{opt}} \coth(\gamma_N e V_{\text{opt}}) = -\gamma_N \Delta \frac{d \ln[K_1(\gamma_N \Delta)]}{d(\gamma_N \Delta)} - 1. \quad (6)$$

We like to stress that this result is independent of the lead temperature T_S . In the limit $\gamma_N \Delta \gg 1$ and $eV \sim \Delta$ Eq. 6 simplifies again considerably to

$$e V_{\text{opt}} = \Delta - k_B T_N \ln 2 \approx \Delta - 0.69 k_B T_N. \quad (7)$$

In Fig. 2 we plot both the numerical solution of (6) and its approximation (7). Up to $k_B T_N \approx 0.3\Delta$ the approximation works nicely thus covering the relevant temperature range (see next paragraph). It is difficult to observe this shift in the experimental data,⁴ since it corresponds to maximal 28 μV only.

In Fig. 3 the heat current (4) using the optimal bias voltage V_{opt} of (6) is shown in comparison with both experimental data and the simpler approximation (5). The maximum of the heat current is found at $k_B T_N \leq 0.23\Delta$ always. Therefore (7) is a practical approximation under relevant conditions as outlined above. Whereas Eq. 5 yields a useful rule of thumb, the numerical solution is rather convincing. Both the optimal temperature and the maximal heat current are determined satisfactory for higher temperature. For lower temperature, however, we observe an increasing deviation. This deviation can not be due to our approximation (3), which improves with decreasing temperature. According to Ref. 4 also the

thermometer as such is not responsible for those discrepancies. We attribute the deviation to rising nonequilibrium effects,² i.e. a non-Fermi like energy distribution of the electrons on the island. In Ref. 2 a value of 100 mK is given as a lower limit of the equilibrium description. The exact value, however, depends on the specific sample layout. It is reasonable to expect an increased limit for the experiment under consideration since the temperature reduction is considerably larger and consequently the nonequilibrium effect becomes more pronounced.

Finally, we are going to discuss an estimate of the lower limit of the electron temperature T_N based on (4). It is assumed that the heating of the electrons on the island is only due to phonon coupling⁴ and follows¹¹

$$P_{\text{el-ph}} = \Sigma \Omega (T_S^5 - T_N^5) \quad (8)$$

with the island volume Ω and a material dependent prefactor Σ . Eq. 8 implies the assumption that the electrons in the leads are in thermal equilibrium with the phonons and the phonon temperature is constant throughout the whole device. For the stationary situation at optimal bias, $P(V_{\text{opt}}) = P_{\text{el-ph}}$, follows a relation between T_N and T_S in terms of Eqs. 4, 6, and 8. Simpler is the treatment using (5) and (7) instead of (4) and (6), respectively, which results in the expression

$$\left(\frac{k_B T_S}{\Delta}\right)^5 = \left(\frac{k_B T_N}{\Delta}\right)^5 + A \left(\frac{k_B T_N}{\Delta}\right)^{3/2} \quad (9)$$

with $A = (\pi \ln 2)^{3/2} / (2\pi) \Delta^2 / (e^2 R \Sigma \Omega) (k_B / \Delta)^5$. For the maximum temperature reduction, $T_S - T_N$, (9) yields

$$\left(\frac{k_B T_{S,\text{opt}}}{\Delta}\right)^4 = \left(\frac{k_B T_{N,\text{opt}}}{\Delta}\right)^4 + 0.3 A \left(\frac{k_B T_{N,\text{opt}}}{\Delta}\right)^{1/2} \quad (10)$$

for the optimal values of $T_{N,S}$. Using a further approximation, $T_{N,\text{opt}} \ll T_{S,\text{opt}}$, we find from (9) and (10)

$$\begin{aligned} T_{N,\text{opt}} &\approx 0.3^{10/7} A^{2/7} \approx 0.179 A^{2/7}, \\ T_{S,\text{opt}} &\approx 0.3^{3/7} A^{2/7} \approx 0.597 A^{2/7}. \end{aligned} \quad (11)$$

The last approximation reveals an interesting uniform relation $T_{N,\text{opt}}/T_{S,\text{opt}} \approx 0.3$ for the optimal working point of the refrigerator, independent of all device parameters. Indeed, the optimal values of the experiment, $T_{N,\text{opt}} \approx 100$ mK and $T_{S,\text{opt}} \approx 300$ mK, almost meet this universal ratio. Furthermore, since the figure of the ratio assembles from the general exponents 3/2 and 5 only, it is expected to be right beyond the range of our approximation.

In Fig. 4 the numerical solution of $P(V_{\text{opt}}) = P_{\text{el-ph}}$ in terms of Eqs. 4, 6, and 8 is compared with the approximation (9) and the experimental data. Similarly to the discussion above we attribute the deviations at low temperature to the manifestation of nonequilibrium. Otherwise we notice fair agreement of the numerical solution

and its approximation as long as the temperature is not too high. In comparison with the experiment we compute $T_{N,\text{opt}} \approx 75$ mK and $T_{S,\text{opt}} \approx 250$ mK from (11). This values are somewhat lower than the measured data (see last paragraph).

IV. CONCLUSION

In this paper electron refrigeration by means of tunnel junctions is studied theoretically. An approximation of the original expression of the heat current across those junctions enables a closed analytic formula for this quantity. Based on this formula several features of the refrigerator are discussed. The optimal bias voltage is determined and the proportionality of the corresponding heat current to $T_N^{3/2}$ is confirmed. The maximal difference of the electron temperature in the leads, T_S , and the island, T_N , is discussed in stationary regime. Analytic approximations to the optimal values of these temperatures are derived and an universal ratio $T_{N,\text{opt}}/T_{S,\text{opt}} = 0.3$ is found. All results are discussed in comparison with a recent experiment. The investigation of nonequilibrium effects, that occur at very low temperature, remains an interesting open problem.

ACKNOWLEDGMENTS

We are indebted to M. M. Leivo and J. P. Pekola for discussion on this subject and for leaving their paper to us prior to publication. One of us (HOM) gratefully acknowledges financial support by Deutscher Akademischer Austauschdienst.

¹ hom@phys.unit.no.

² M. Nahum, T. M. Eiles, and J. M. Martinis, Appl. Phys. Lett. **65**, 3123 (1994).

³ J. Pekola, K. Hirvi, J. Kauppinen, and M. Paalanen, Phys. Rev. Lett. **73**, 2903 (1994).

⁴ M. M. Leivo, J. P. Pekola, and D. V. Averin, Appl. Phys. Lett. **68**, 1996 (1995), cond-mat/9511127.

⁵ D. V. Averin and K. K. Likharev, J. Low Temp. Phys. **62**, 345 (1986).

⁶ A. Bardas and D. V. Averin, Phys. Rev. B **52**, 12873 (1995), cond-mat/9505097.

⁷ J. Oswald, <http://nahum-www.harvard.edu/expts/noneq.html> (unpublished).

⁸ W. Krech and H.-O. Müller, Mod. Phys. Lett. B **8**, 605 (1994).

⁹ F. Oberhettinger and L. Badii, *Tables of Laplace Transforms* (Springer, Berlin, Heidelberg, 1973).

- ¹⁰ M. Abramowitz and I. A. Stegun, *Pocketbook of Mathematical Functions* (Harri Deutsch, Thun, 1984).
¹¹ F. C. Wellstood, C. Urbina, and J. Clarke, Phys. Rev. B **49**, 5942 (1994).

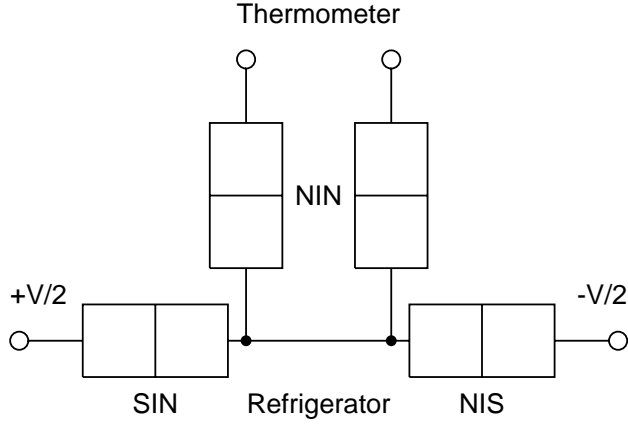


FIG. 1. Combination of refrigerator and thermometer, both based upon tunnel junctions. The horizontally shown refrigerator consists of a superconductor-insulator-normal-metal (SIN) junction to the left and a NIS-junction to the right biased by a voltage V . The vertically displayed thermometer tests the electron temperature of the island in the middle by means of two NIN-junctions.

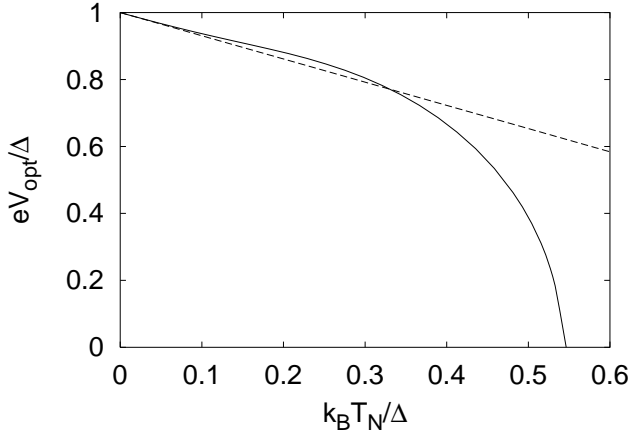


FIG. 2. Optimal bias voltage V_{opt} in dependence on the electron temperature on the island T_N . The solid curve displays the numerical solution of (6) and the dashed line its approximation (7).

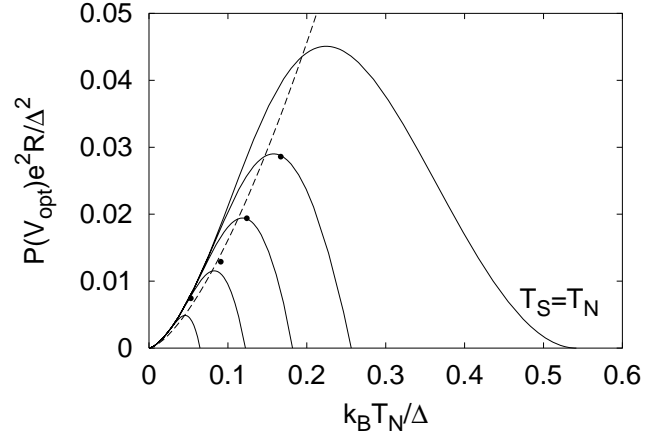


FIG. 3. The maximal heat current $P(V_{\text{opt}})$ as a function of the electron temperature T_N . The solid lines correspond to different ratios T_S/T_N of the electron temperature in the leads and the island. For the uppermost curve this ratio is 1, whereas it corresponds to the values of the experiment for the other curves. The dashed line shows Eq. 5, and the dots (•) correspond to the values of the experiment.

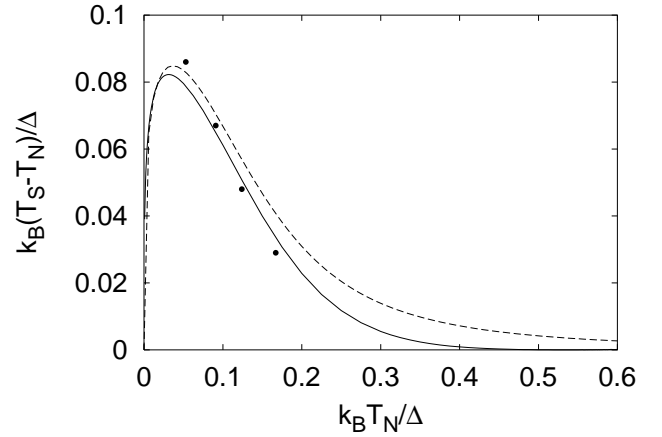


FIG. 4. Temperature reduction $T_S - T_N$ versus T_N . The solid curve corresponds to the numerical procedure described in the text, whereas the dashed line is a plot of (9). The symbols (•) are again the data of the experiment.